Fluoride anion complexation and transport using a stibonium cation stabilized by an intramolecular $P=O \rightarrow Sb$ pnictogen bond

Vanessa M. Gonzalez, Gyeongjin Park, Mengxi Yang, François P. Gabbaï*

Department of Chemistry, Texas A&M University, College Station, Texas 77843-3255, USA

Supporting Information Placeholder

ABSTRACT: We describe the synthesis of $[o-Ph_2P(=O)(C_6H_4)SbPh_3]^+$ ($[\mathbf{2}]^+$), an intramolecularly base-stabilized stibonium Lewis acid which was obtained by reaction of $[o-Ph_2P(C_6H_4)SbPh_3]^+$ with NOBF₄. This cation reacts with fluoride anions to afford the corresponding fluorostiborane $o-Ph_2P(=O)(C_6H_4)SbFPh_3$, the structure of which indicates a strengthening of the P=O \rightarrow Sb interaction. When deployed in fluoride-containing POPC unilamellar vesicles, $[\mathbf{2}]^+$ behaves as a potent fluoride anion transporter whose activity greatly exceeds that of $[Ph_4Sb]^+$.

The Lewis acidity and fluoride affinity of pnictogen derivatives in the +V oxidation state is well-known property that comes to light in the facile conversion of the pentafluorides into the corresponding hexafluoro-pnictogenates. As previously explained, SbF₅ is the most fluoridophilic representative of this series, 1 an attribute that has been exploited for the generation of superacids. 2 High fluoride anion affinity is also displayed by organoantimony(V) derivatives such as $[Ph_4Sb]^+$ (A, Figure 1) which was used early on for the complexation and phase transfer of aqueous fluoride anions. 3 These seminal results led to the advent of additional examples of such tetraarylstibonium cations, including $[AntSbPh_3]^+$ (B, Ant = 9-anthracenyl) which functions as a water-compatible fluorescence turn-on sensor capable of detecting ppm levels of fluoride. 4

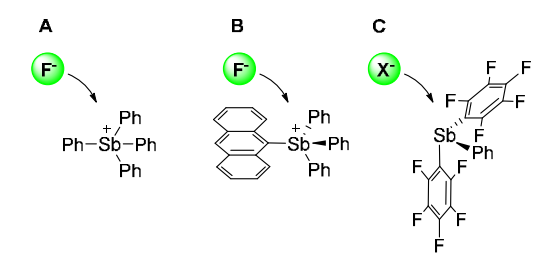


Figure 1: Structure of antimony(V) compounds used as fluoride anion transporters.

More recently, our work has also shown that such derivatives promote the transport of fluoride anions across artificial phospholipid bilayer membranes.⁵ Such anion transport

properties are interestingly also observed in the case of electron-deficient stibines bearing the pentafluorophenyl substituent (C).⁶ Apart from these precedents, no other type of antimony derivatives have been investigated as anion transporters, although several additional examples have been used in anion sensing studies.⁷ To paint a fuller picture of the potential that main group compounds present in the area of anion tranport,^{6,8} we have decided to investigate base-stabilized stibonium cations. Based on the known affinity of stibonium cations for phosphine oxides,⁹ we now report on the synthesis and study of a stibonium cation stabilized by an intramolecular P=O→Sb pnictogen bond, a term often used to describe dative bonding involving group 15 acceptors.¹⁰

We selected the known stibonium bromide [o- $Ph_2P(C_6H_4)SbPh_3[Br]$ ([1][Br])¹¹ and subjected it to a 30% aqueous hydrogen peroxide solution in CH2Cl2. While the emergence of a ³¹P{¹H} NMR signal at 31.3 ppm suggested the formation of the corresponding phosphine oxide, the reaction was sluggish, only affording partial conversion after 12 hours. The relatively low conversion observed in this reaction may result from donor-acceptor bonding between the phosphorus atom and the stibonium center, which tames the reactivity of the phosphorus center. Indeed, prior Natural Bond Orbital calculations have shown the presence of a lp(P) \rightarrow σ^* (Sb-C) interaction associated with a stabilization energy E_{del} of 8.3 kcal/mol. To overcome this passivating interaction, we resorted to the more potent oxidant NOBF₄ which has previously been used to access phosphine oxides. 12 We were encouraged to find that, under ambient conditions, [1]Br was cleanly and quantitatively converted into the corresponding phosphine oxide ([2]BF4) when treated with NOBF₄ in CH₂Cl₂/H₂O (10/1 v/v)(Scheme 1). This new phosphine oxide stibonium salt has been characterized by elemental analysis, mass spectrometry, and NMR spectroscopy. Comparison of the ¹H NMR spectra of [1]Br and [2][BF₄] showed an overall downfield shift indicative of a slight deshielding induced by the phosphine-oxide moiety. The ³¹P NMR resonance of [2][BF₄] at 31.3 ppm appears significantly deshielded when compared to that of Ph₃PO (23.2 ppm) suggesting possible coordination of the PO functionality to the antimony center. To more definitively address this structural feature, we attempted the crystallization of this new salt.

Scheme 1. Synthesis of [2]BF4 using NOBF4.

Single crystals of [2][BF4] were obtained by vapor diffusion of Et_2O into a saturated $CDCl_3$ solution of the salt. Analysis of these crystals by X-ray diffraction afforded the structure shown in Figure 2. The O-Sb distance of 2.4315(13) Å, which falls between the values of 2.406(2) Å and 2.449(1) Å respectively determined for the trimethylphosphine oxide and 4-methylpyridine-N-oxide adducts of $[SbPh_4]^+$,9a is consistent with the intramolecular coordination of the phosphine oxide functionality of [2]+ to the antimony center. This view is supported by the nearly linear O-Sb-C₁₃ angle of 176.28(5)° and the resulting trigonal bipyramidal coordination geometry of the antimony center. When compared to the value of 1.484(1) Å measured in Ph_3PO ,13 the P-O bond of [2]+ (1.5113(12) Å) displays significant elongation providing another evidence for the presence of a P=O→Sb linkage.

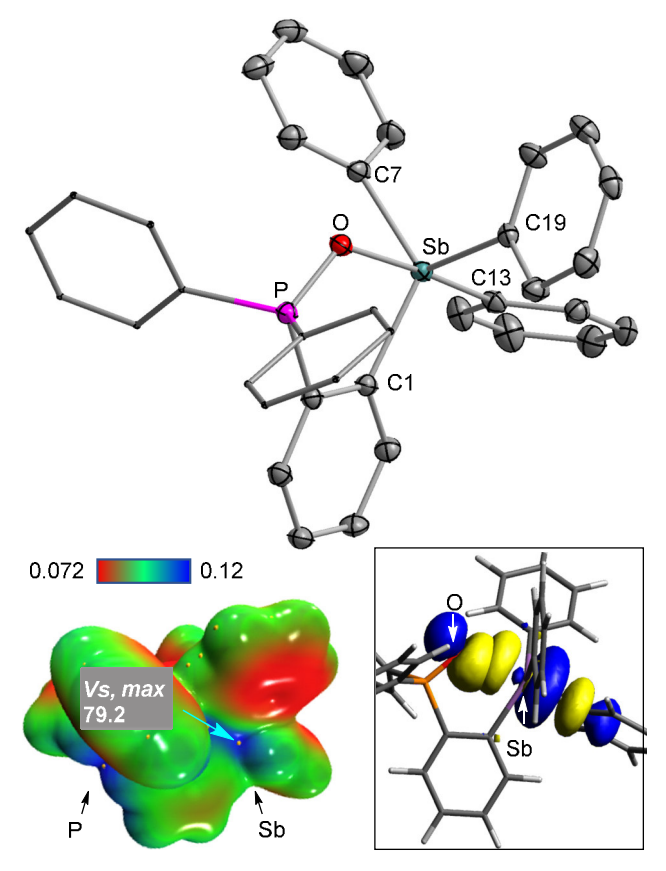


Figure 2. Top: Structure of [2][BF4] with ellipsoids drawn at the 50% probability level. The hydrogen atoms and the tetrafluoroborate counter anion are omitted for clarity. Selected bond lengths (Å) and angles (deg): P-O = 1.5113(12), O-Sb = 2.4315(13), O-Sb-C13 = 176.28(5), C7-Sb-C19 = 111.23(6), C19-Sb-C1 = 115.71(6), C1-Sb-C7 = 123.24(6). Bottom left: Electrostatic potential map (ESP) of [2]+ (surface isovalue = 0.001 a.u.) showing

the location the point featuring V_s ,max (in kcal mol⁻¹). Bottom right: NBO contour plot shown one of the lp(O) $\rightarrow \sigma^*$ (Sb-C) interactions in [2] $^+$.

The structure of [2]+ has been computationally optimized and analyzed using the Natural Bond Orbital (NBO) method which confirms the presence of several lp(O) $\rightarrow \sigma^*$ (Sb-C) interaction, one of which is illustrated in Figure 2. Collectively, these interactions stabilize the molecule by E_{del} = 51.9 kcal/mol indicating significant charge transfer from the phosphine oxide to the antimony center. To understand if the formation of this P=O→Sb bridge affects the electrophilic character of the antimony(V) center, we analyzed the ESP map of [2]+. This analysis indicates that the maximum potential value $(V_{S,max})$ is found about the antimony atom, a characteristic shared with previously investigated stibonium cations such as [Ph₄Sb]⁺.^{5a} The location of this point of maximum potential serves to define the site of highest Lewis acidity also referred to as the σ -hole present at the group 15 element. When compared to that of $[Ph_4Sb]^+$ ($V_{S,max} = 93.9$ kcal mol⁻ 1),5a the $V_{S,max}$ value of 79.2 kcal mol-1 calculated for [2]+ is substantially lower, suggesting partial quenching of the σ hole as the result of the P=O→Sb interaction. A similar partial quenching of the σ -hole was proposed for [o-PhS(C₆H₄)SbPh₃]⁺ due to the presence of a S→Sb interaction.5a

Next, it became important to determine if the above mentioned reduction in the depth of the σ -hole in [2]* would negatively affect the anion binding properties of this derivative. Given our longstanding interest in the development of fluoride anion sensors and/or transporters, a 8/2 (v/v) THF/water solution of [2][BF₄] was titrated with KF. ³¹P NMR monitoring showed a progressive upfield shift of the resonance from 30 ppm to 27 ppm. Fitting the resulting data to a 1:1 binding isotherm afforded a binding constant of 1.0±0.1 x10⁴ M⁻¹. Interestingly, repeating this experiment with KCI instead of KF showed no evidence of binding. To verify the formation of this fluoride adduct (2-F), its isolation was attempted. Treatment of [2][BF₄] with KF in MeOH leads to the precipitation of 2-F (Figure 3). The ¹⁹F NMR spectrum of 2-F displays a resonance at -61.1 ppm, a value comparable to that of other fluorostiboranes. The ³¹P NMR resonance at 26.9 ppm is close to that observed at the endpoint of the above-described titration.

Single crystals of this compound could be easily obtained by diffusion of Et_2O into a CH_2Cl_2 solution of **2**-F. Subsequent X-ray diffraction analysis indicates that **2**-F is indeed a fluoride adduct as illustrated in Figure 3. The antimony atom adopts a distorted octahedral geometry with the fluoride anion occupying a position cis from the intramolecularly coordinated phosphine oxide moiety. The resulting Sb-F bond length of 2.028(3) Å is comparable to that measured for other fluorostiboranes.⁴ The Sb-O bond length of 2.341(4) Å is significantly shorter than the value of 2.4315(13) Å measured for [**2**][BF₄]. This shortening may come across as counterintuitive since one might expect that coordination of a fluoride anion would reduce the Lewis acidity of the antimony center and decrease the strength of the P=O \rightarrow Sb interaction.

However, Gutmann has explained that increasing the coordination number induces a spillover of the electron density on the ligand resulting in a net decrease of the density on the central atom.¹⁴ In other words, an increase in the coordination number of a main group Lewis acid leads to increased ionicity of the bonding. This phenomenon, which has been coined by Denmark as the "Lewis base activation of a Lewis acid"15 is likely responsible for the observed contraction of the O-Sb distance on going from [2]+ to 2-F. The ionicity of the Sb-C bonds has been assessed using NBO calculations which show an increased polarization of Sb-C bonds, with bonding pair toward the carbon atom in 2-F (see SI). The resulting stabilization of the P=O→Sb bridge is also supported by the E_{del} value of 55.7 kcal/mol obtained upon zeroing the Kohn-Sham matrix elements corresponding to the O→Sb donor-acceptor interactions. Indeed, this value is notably higher than in [2]⁺ (E_{del} = 51.9 kcal/mol).

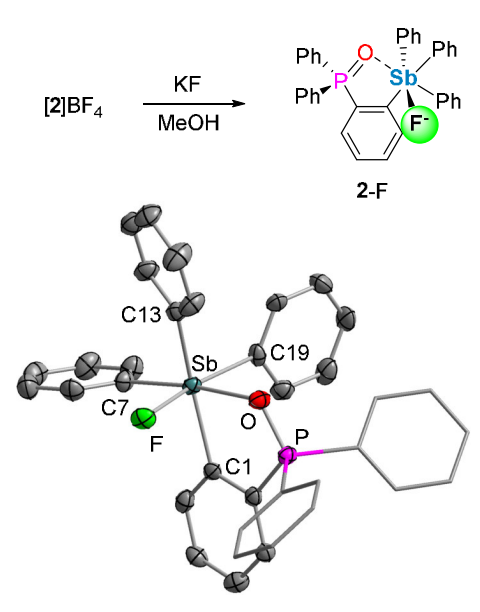


Figure 3. Crystal Structure of **2**-F with the ellipsoids drawn at 50% probability level and hydrogen atoms omitted for clarity. Select bond lengths (Å) and angles (deg): P-O = 1.520(4), O-Sb = 2.341(4), Sb-F = 2.028(3), O-Sb-C7 = 172.86(17), F-Sb-C13 = 82.76(17), C13-Sb-C19 = 97.5(2), C19-Sb-C1 = 93.92(19), C1-Sb-F = 82.61(15).

Encouraged by the formation of 2-F and contemplating possible applications in radiofluorination chemistry,16 we decided to test whether [2]+ could also be used as a fluoride anion transporter. Using a POPC vesicle-based assay that we have developed in the past^{5a} and a fluoride ion selective electrode,17 the fluoride transport activity of [2][BF4] was determined and compared to that of [Ph₄Sb]⁺ as a model compound. After 270 seconds, [2]BF4 had resulted in approximately 83% fluoride efflux compared to the 29% fluoride efflux of [Ph₄Sb]OTf (Figure 4). The transport activity of triphenylphosphine oxide was almost indistinguishable from the DMSO control supporting the assertion that the fluoride bonds to the antimony(V) center. The transport activity between [2]BF₄ and [Ph₄Sb]OTf was quantitatively compared by calculating the initial transport rate for the average of two experiments. The k_{int} for [2]BF₄ was approximately five times greater than the kint for [Ph4Sb]OTf. Additionally, the EC50(F-),

which is the mol % of transporter needed for 50% transport activity, for [2]BF₄ was determined to be 0.24 (±0.03) mol% which is lower than the previously reported EC₅₀(F-) value for [Ph₄Sb]OTf (6.91 (±0.70) mol % in EYPC vesicles) but on par with that of **B** (0.41(±0.05) mol % in EYPC vesicles).5b We attribute the elevated fluoride anion transport properties of [2]BF4 to its increased hydrophobicity. The hydrophobicity of the compound was approximated by the computed n-octanol/water coefficient (log K_{ow}) of [2]BF₄ (log K_{ow} = 7.20) which is significantly higher than that of [Ph₄Sb]OTf (log K_{ow} = 4.19).18 It is important to note that [Ph₄Sb]⁺ is slightly more Lewis acidic than [2]⁺ as shown by the FIA calculations which are 133.0 kcal/mol and 125.0 kcal/mol, respectively. Thus, the higher transport properties of [2]BF4 most likely result from the increased hydrophobicity of the compound. The lower FIA of [2]+ also suggests that the intramolecular coordination of the phosphine oxide to the antimony atom may quench the Lewis acidity of the antimony center. This conclusion may come across as paradoxical since, as described above, fluoride coordination to [2]+ enhances the intramolecular O→Sb interaction.

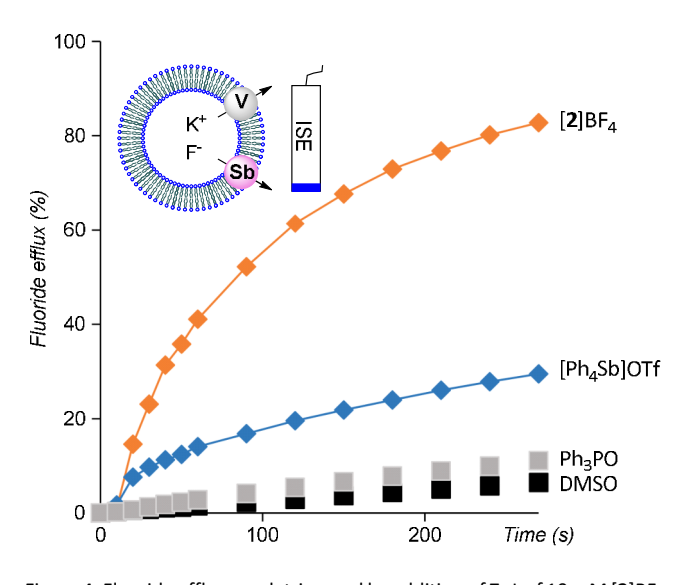


Figure 4. Fluoride efflux graph triggered by addition of 7μ L of 10 mM [2]BF₄ and [Ph₄Sb]OTf in DMSO solution. The $K_{ini.}$ is the initial efflux rate (% s^{-1}).

The present results indicate that base-stabilized stibonium cations are potent Lewis acids¹⁹ that readily capture and transport fluoride anions across phospholipid membranes. Since the nature of the Lewis base could be easily varied, we propose that the transport properties of tetraaryl stibonium cations could be easily adjusted by changing the lipophilicity of the Lewis base. This idea is the subject of current investigations in our laboratory.

Conflicts of interest

There are no conflicts to declare

Acknowledgements

This work was supported by the National Science Foundation (CHE-2108728), the Welch Foundation (A-1423), and Texas A&M University (Arthur E. Martell Chair of Chemistry).

References

- 1. a) I. Krossing and I. Raabe, Chem. Eur. J., 2004, 10, 5017-5030; b) J. Moc and K. Morokuma, J. Mol. Struct., 1997, 436-437, 401-
- 2. a) G. A. Olah, G. Klopman and R. H. Schlosberg, J. Am. Chem. Soc., 1969, 91, 3261-3268; b) G. A. Olah and R. H. Schlosberg, J. Am. Chem. Soc., 1968, 90, 2726-2727; c) G. A. Olah, J. Org. Chem., 2005, 70, 2413-2429.
- 3. a) L. H. Bowen and R. T. Rood, J. Inorg. Nucl. Chem., 1966, 28, 1985-1990; b) M. Jean, Anal. Chim. Acta, 1971, 57, 438-439; c) K. D. Moffett, J. R. Simmler and H. A. Potratz, Anal. Chem., 1956, 28,
- 4. a) I.-S. Ke, M. Myahkostupov, F. N. Castellano and F. P. Gabbaï, J. Am. Chem. Soc., 2012, 134, 15309-15311; b) M. Hirai, M. Myahkostupov, F. N. Castellano and F. P. Gabbaï, Organometallics, 2016, 35, 1854-1860.
- 5. a) G. Park and F. P. Gabbaï, *Chem. Sci.*, 2020, **11**, 10107-10112; b) G. Park, D. J. Brock, J.-P. Pellois and F. P. Gabbaï, Chem, 2019, 5,
- 6. L. M. Lee, M. Tsemperouli, A. I. Poblador-Bahamonde, S. Benz, N. Sakai, K. Sugihara and S. Matile, J. Am. Chem. Soc., 2019, 141,
- 7. a) A. M. Christianson and F. P. Gabbaï, in Main Group Strategies towards Functional Hybrid Materials, eds. T. Baumgartner and F. Jaekle, John Wiley & Sons Ltd, Hoboken, NJ, 2018, pp. 405-432; b) A. Kumar, M. Yang, M. Kim, F. P. Gabbaï and M. H. Lee, Organometallics, 2017, 36, 4901-4907; c) A. M. Christianson, E. Rivard and F. P. Gabbaï, *Organometallics*, 2017, **36**, 2670-2676; d) A. M. Christianson and F. P. Gabbaï, Organometallics, 2017, 36, 3013-3015; e) A. M. Christianson and F. P. Gabbaï, J. Organomet. Chem., 2017, 847, 154-161; f) A. M. Christianson and F. P. Gabbaï, Chem. Commun., 2017, 53, 2471-2474; g) M. Hirai and F. P. Gabbaï, Angew. Chem. Int. Ed., 2015, 54, 1205-1209; h) M. Hirai and F. P. Gabbaï, Chem. Sci., 2014, 5, 1886-1893; i) C. R. Wade and F. P. Gabbaï, Z. Naturforsch., B: J. Chem. Sci., 2014, 69, 1199-1205; j) C. R. Wade, I.-S. Ke and F. P. Gabbaï, Angew. Chem. Int. Ed., 2012, 51, 478-481; k) C. R. Wade and F. P. Gabbaï, Organometallics, 2011, 30, 4479-4481; I) T.-P. Lin, R. C. Nelson, T. Wu, J. T. Miller and F. P. Gabbaï, Chem. Sci., 2012, 3, 1128-1136.
- 8. a) A. J. Plajer, J. Zhu, P. Pröhm, F. J. Rizzuto, U. F. Keyser and D. S. Wright, J. Am. Chem. Soc., 2020, 142, 1029-1037; b) A. J. Plajer, J. Zhu, P. Proehm, A. D. Bond, U. F. Keyser and D. S. Wright, J. Am. Chem. Soc., 2019, 141, 8807-8815; c) S. Benz, M. Macchione, Q. Verolet, J. Mareda, N. Sakai and S. Matile, J. Am. Chem. Soc., 2016, 138, 9093-9096; d) A. Vargas Jentzsch, D. Emery, J. Mareda, S. K. Nayak, P. Metrangolo, G. Resnati, N. Sakai and S. Matile, Nat. Commun., 2012, 3, 905.
- 9. a) A. P. M. Robertson, S. S. Chitnis, H. A. Jenkins, R. McDonald, M. J. Ferguson and N. Burford, Chem. Eur. J., 2015, 21, 7902-7913; b) A. P. M. Robertson, N. Burford, R. McDonald and M. J. Ferguson, Angew. Chem. Int. Ed., 2014, 53, 3480-3483; c) D. Tofan and F. P. Gabbaï, Chem. Sci., 2016, 7, 6768-6778; d) M. Yang, D. Tofan, C.-H. Chen, K. M. Jack and F. P. Gabbaï, Angew. Chem. Int. Ed., 2018, **57**, 13868-13872; e) Y. H. Lo and F. P. Gabbaï, *Angew. Chem. Int.* Ed., 2019, 58, 10194-10197; f) J. E. Smith, H. Yang and F. P. Gabbaï, Organometallics, 2021, DOI: 10.1021/acs.organomet.1c00371, published online, see DOI:10.1021/acs.organomet.1021c00371. 10. K. T. Mahmudov, A. V. Gurbanov, V. A. Aliyeva, G. Resnati and
- A. J. L. Pombeiro, Coord. Chem. Rev., 2020, 418, 213381.
- 11. M. Yang, M. Hirai and F. P. Gabbaï, Dalton Trans., 2019, 48, 6685-6689.
- 12. G. A. Olah, B. G. B. Gupta and S. C. Narang, J. Am. Chem. Soc., 1979, **101**, 5317-5322.

- 13. A. L. Spek, Acta Crystallographica Section C, 1987, 43, 1233-
- 14. V. Gutmann, Rev. Roum. Chim., 1977, 22, 619.
- 15. S. E. Denmark and T. Wynn, J. Am. Chem. Soc., 2001, 123, 6199-6200.
- 16. K. Chansaenpak, B. Vabre and F. P. Gabbaï, Chem. Soc. Rev., 2016, **45**, 954-971.
- 17. H. J. Clarke, E. N. Howe, X. Wu, F. Sommer, M. Yano, M. E. Light, S. Kubik and P. A. Gale, J. Am. Chem. Soc., 2016, 138, 16515-16522.
- 18. G. Park, D. J. Brock, J. P. Pellois and F. P. Gabbai, Chem, 2019, **5**, 2215-2227.
- 19. R. Arias-Ugarte, D. Devarajan, R. M. Mushinski and T. W. Hudnall, Dalton Trans., 2016, 45, 11150-11161.